

## Automated protective cell detection for photovoltaic panels using drone

by C. Kim\*, J.-S. Choi\*\*, S. Perilli\*\*\*, S. Sfarra\*\*\*\* and E.-J. Kim\*\*†

\* Department of Architectural Engineering, Inha University, Incheon 22212, Korea

\*\* Department of Smart City Engineering, Graduate School of Inha University, Incheon 22212, Korea

\*\*\* Independent Researcher, Santa Rufina di Roio – L'Aquila I-67100, Italy

\*\*\*\* Department of Industrial and Information Engineering and Economics, University of L'Aquila, L'Aquila I-67100, Italy

† Corresponding author: [ejkim@inha.ac.kr](mailto:ejkim@inha.ac.kr)

### Abstract

The objective of this study was to propose a method for detecting photovoltaic cells modified with protective coatings. To detect those modified cells among cells indicating slight temperature differences, the local maximum temperature was obtained from consecutively acquired thermal images. The performance of the proposed method was validated through field experiments. Results from the experiments showed that all cells coated with a protective material were successfully detected using the proposed method. Furthermore, those cells could be automatically detected despite the slight temperature difference among them.

### 1. Introduction

Photovoltaic (PV) panels are exposed to harsh environments by their genuine characteristics and being installed outdoors. Harsh environments directly damage PV panels and degrade their performance [1]. For example, moisture ingress reduces the life of PV modules through corrosion and material deterioration [2]. In addition, sand particles may collide with the PV panel due to wind, which may result in scratches on the PV panel [3]. Accordingly, various companies are manufacturing transparent coating products that can increase the resistance of PV panels to moisture [4–6] and scratches [7]. However, if the panel is coated, some of the protective material may be eroded over time, whereas some areas may not be coated because of error. Hence, the area requiring surface coating should be verified and re-coated if necessary. However, the coated area is difficult to inspect visually because the protective material is transparent.

Recently, drones equipped with thermal imaging cameras have been employed to automatically detect various problems that may occur on the surface of objects [8]. In particular, previous studies showed that various defects in PV panels are detectable using infrared thermography [9,10]. In those studies, the detection of defects that differ by more than 10 °C compared with those in normal areas, such as hotspots, was prioritized. However, the coating applied to the PV panel to be detected in this study did not indicate a significant temperature difference, such as a difference of less than 5 °C from its surrounding.

Therefore, a method for detecting modified cells on a PV panel (i.e., cells coated with a protective material) using continuous aerial infrared thermography was devised in this study. The scope of the research subject was limited to modified cells whose temperature was higher than the surrounding temperature. The remainder of this paper is organized as follows: the framework and details of the proposed method for detecting modified cells on a PV panel are provided in Section 2. In Section 3, the experimental validation of the proposed method based on its performance is presented. Finally, in Section 4, the conclusion of this study and directions for future research are presented.

### 2. Proposed modified cell detection method

The modified cell with a protective coating typically exhibits a small temperature difference compared to the surroundings, and it is not a common detection case with the thermography as the hotspot detection. In this study, the modified cells were detected by identifying an area that was relatively high in temperature compared with the area surrounding the surface of the PV panel under investigation using a continuous recording of infrared images. First, thermal images were continuously acquired from the PV panel using a drone equipped with a thermal imaging camera. Recently manufactured thermal imaging cameras can simultaneously acquire both visible and thermal images. Because a visible image contains color information, it can be used for image processing. However, since the thermal and visible images are not accurately aligned, registration must be performed between them. In the thermal image, a median filter is applied as a preprocessing step to remove noise in the thermal image. Subsequently, the PV cell, which was the region of interest, was detected only from the registered visible image. The PV cell detection involves PV frame detection and PV cell masking. In PV frame detection, the PV frame is detected in the visible image. Subsequently, a PV cell mask is obtained based on the PV frame. After applying the mask to the PV cell obtained from the visible image to the thermal image, the modified area is detected based on the temperature in the PV cell area. The modified cell is detected via two steps. First, a region of relatively high temperature is identified. Subsequently, the modified cell is detected based on results obtained by repeatedly performing the preceding process on individual thermal and visible images. Figure 1 shows the modified cell detection method proposed herein.



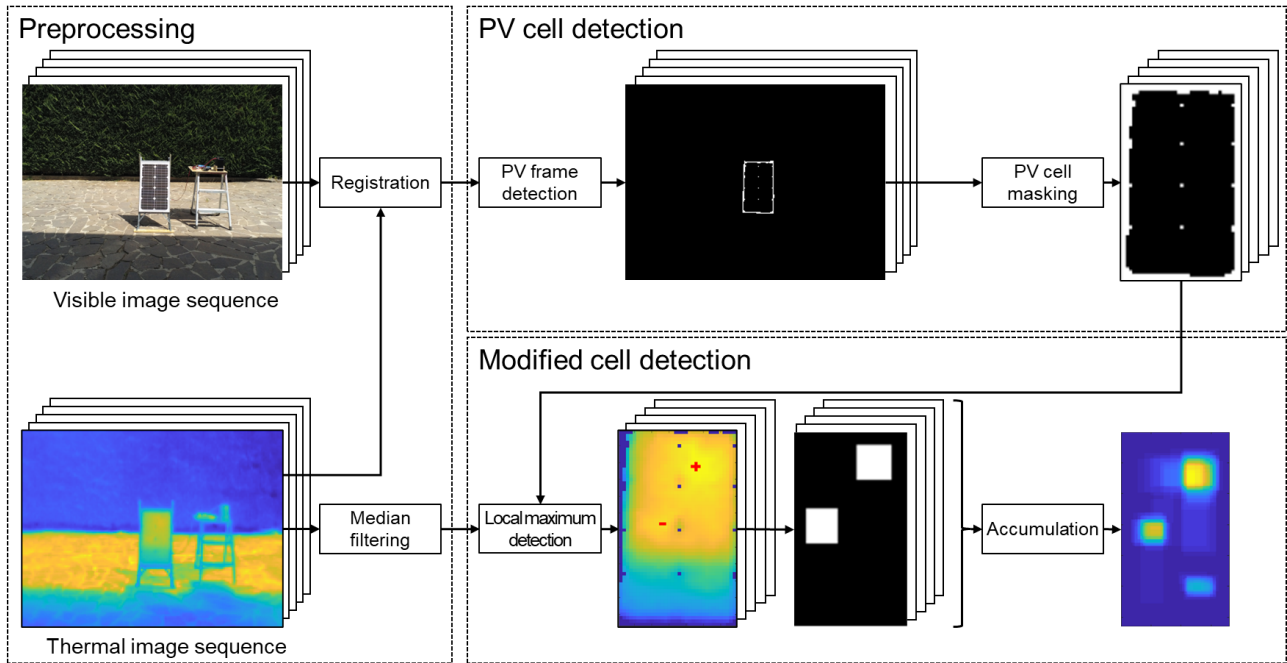
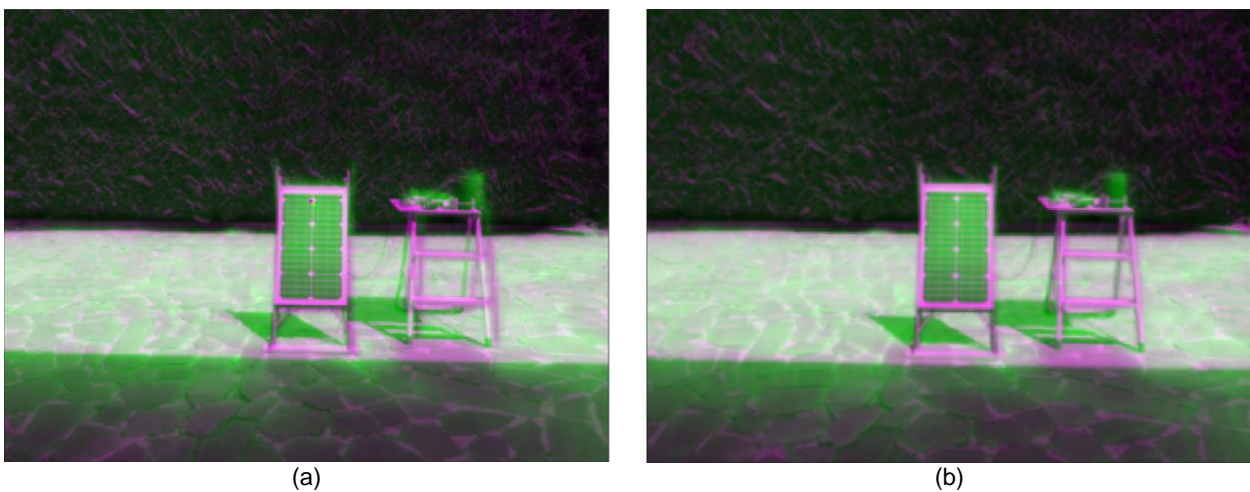


Fig. 1. Automated modified cell detection method

## 2.1. Preprocessing

### 2.1.1. Registration

In this study, intensity-based registration was performed to align the visible and thermal images. Intensity-based registration is a method for determining the best alignment that optimizes a predefined similarity metric. To perform intensity-based registration, a visible image composed of three channels — red (R), green (G), and blue (B) — is first converted into an intensity image. Because the visible image has a higher resolution than the thermal image, the resolution of the visible image is reduced based on that of the thermal image. Subsequently, the similarity between the thermal and visible images is measured using mutual information. Figure 2 shows the registration process between the visible and thermal images. In Fig. 2, the areas in green and magenta represent the intensities of the visible and thermal images, respectively. As shown in Fig. 2(a), the visible and thermal images are not aligned initially. If the position is repeatedly adjusted to maximize the mutual information, the visible image becomes aligned with the thermal image, as shown in Fig. 2(b).



(a) (b)  
Fig. 2. Registration process (a) initial (b) after optimization

### 2.1.2. Median filtering

To remove noise from the thermal image, a median filter was applied. The median filter can effectively remove salt-and-pepper and speckle noise in the image. Therefore, they are widely used to remove noise from images in various fields. In this study, the median filter was applied as follows: first, a mask representing the range of the neighbor was created. The size of the mask affects the noise-removal performance. In this study, the size of the mask was set to  $3 \times 3$ , and eight pixels from the surroundings were selected as neighbors. Subsequently, the created mask was slid over the entire thermal image; hence, the middle pixel in the mask was replaced with the median of the neighboring pixel values.

## 2.2. PV cell detection

### 2.2.1. PV frame detection

In the visible image, the most unique feature of the PV panels is the frame [Fig. 3(a)]. Therefore, in this study, the frame of the PV panel was first detected to determine the PV module area in a visible image. Two criteria were used for the frame detection of the PV panels. The first criterion was the color of the PV panel frame. The frame of the PV panel showed a unique white color. To detect the frame based on the unique white color, as shown in Fig. 3(b), only pixels above a threshold of 210 were extracted from the R, G, and B channels. This is because objects other than the frame of the PV panel are detected, as shown in Fig. 3(c) when only color is used in the image. To reduce the detection error due to the color criterion, a second criterion was imposed, i.e., the PV panel must be located near the center of the image. Figure 3(d) shows the position range of the PV panel in this study. Results satisfying the two criteria of color and PV panel position are shown in Fig. 3(e). Meanwhile, results that do not correlate with the neighboring pixels are regarded as noise and therefore, removed. The result of overlapping the visible image on the thermal image for frame detection is shown in Fig. 3(f). In Fig. 3(f), the dark area is detected as the frame of the PV panel.

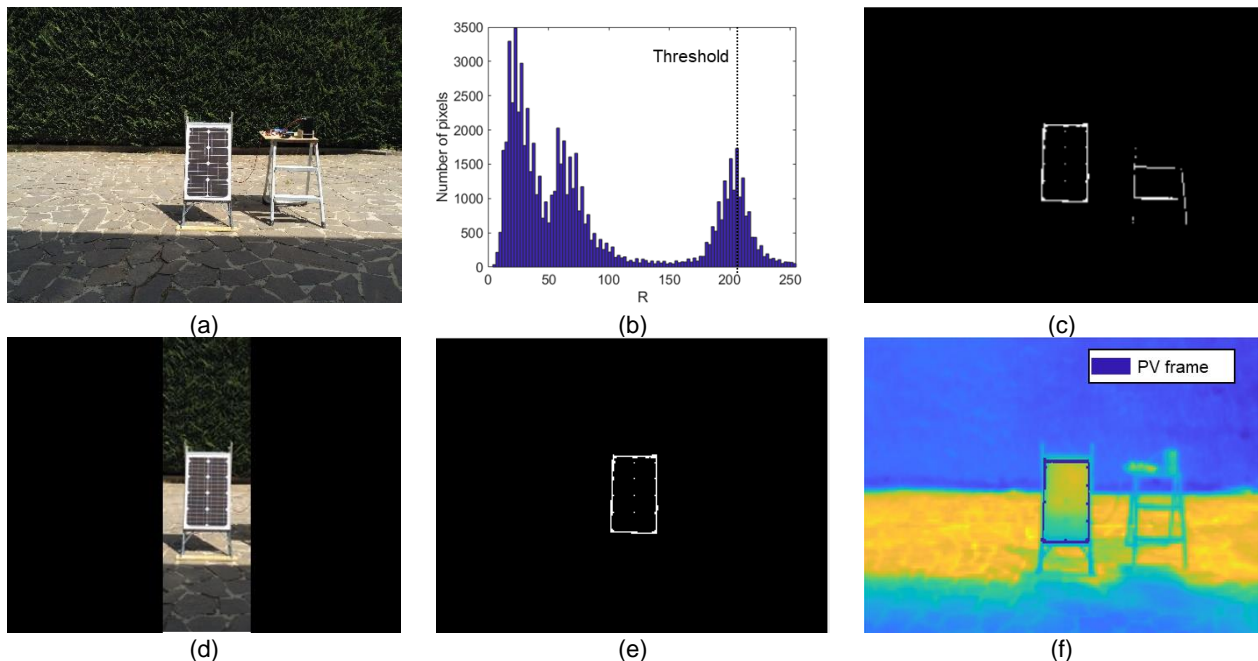


Fig. 3. PV frame detection result (a) visible image (b) histogram of R channel (c) thresholding result (d) range of panel position (e) frame detection result (f) overlap with thermal image

### 2.2.2. PV cell masking

The method for masking the cell region for temperature analysis based on a previously detected frame is as follows: first, the edge pixels of the frame in all horizontal and vertical directions are identified from the frame detection result. An edge pixel indicates the minimum and maximum pixels corresponding to a frame in the same row and column. As shown in Fig. 4(a), one row comprises two edge pixels. Among the pixels located between these two edge pixels, the pixel except the frame is regarded as a PV cell. By repeating this process for all columns and rows, the mask corresponding to the PV cell can be obtained, as shown by the black pixel in Fig. 4(b).

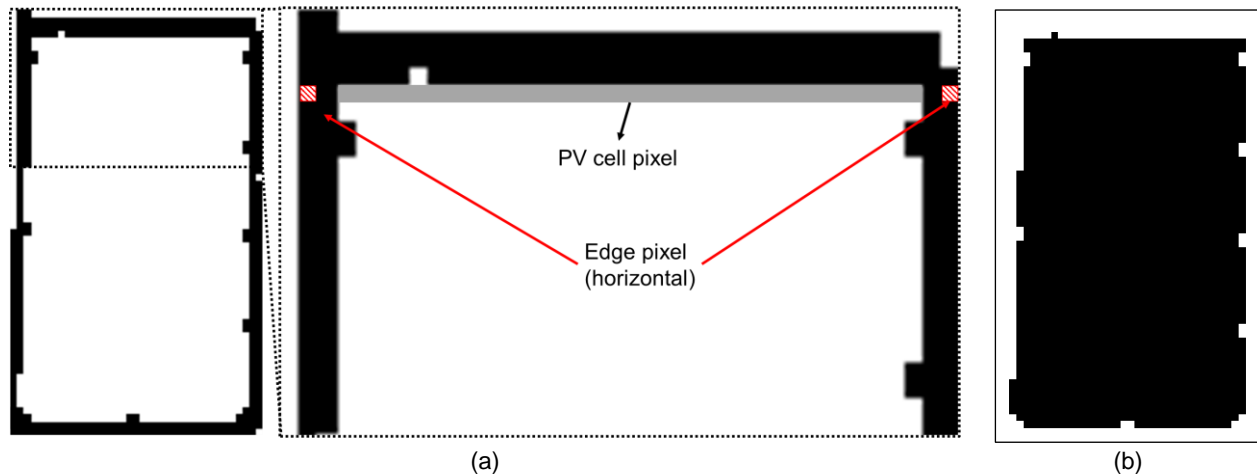


Fig. 4. PV cell masking (a) PV cell masking method (b) mask of PV cell

### 2.3. Protective cell detection

#### 2.3.1. Local maximum area detection

Only the temperature inside the PV cell can be obtained by applying the PV cell mask to the thermal image. In this study, a method to detect a modified cell was devised by analyzing the temperature inside the PV cell. Because the temperature of the modified cell is relatively high compared with that of the uncoated cell, the local maximum temperature was identified as a reference point for the detection of the modified area. The local maximum temperature can be identified by comparing the temperature of each pixel in a thermal image, which is a one-channel image, with those of eight pixels in the upper, lower, left, right, and diagonal positions of the pixel and of the neighboring pixels. If the value of a pixel is greater than those of the eight neighboring pixels, that pixel is regarded as the local maximum pixel. The pixels marked in red in Fig. 5 are pixels regarded as local maximum pixels in the PV cell.

After determining the local maximum pixel, the modified area was detected based on the local maximum pixel. As shown in Fig. 5, the temperature is the highest at the local maximum pixel, whereas it decreases gradually as one departs from the local maximum pixel. In particular, the temperature changes rapidly at a particular point. In this study, the modified area was bounded by those particular points. The proposed modified area detection based on the local maximum pixel was performed as follows: based on the pixel detected as the local maximum, both row and column temperatures were extracted. Subsequently, the temperature difference based on the previous pixel was calculated in the order closest to the local maximum pixel. The first point at which the temperature difference exceeded the threshold was selected as the boundary of the modified area. This process was repeated for the entire local maximum pixel. In this study, the threshold value related to the temperature difference was set as 0.12.

#### 2.3.2. Individual results accumulation

In this study, to improve the accuracy of the modified area detection, an image sequence acquired continuously using a drone was used. In the final process of the proposed method, the modified area detection results of individual images were accumulated. Figures 6(a)–(c) show an example of the detection results of the modified area for three images in the image sequence. Because the image was acquired using a drone, the panel position and angle for each image differed slightly, which caused an error when accumulating the results. Therefore, a template of the same size as that of the image was created, and the ratio and size were corrected using the template. The modified area of each image, created with the same size, was overlaid on one template for a final judgment. Figure 6(d) shows the accumulation results for the three examples.

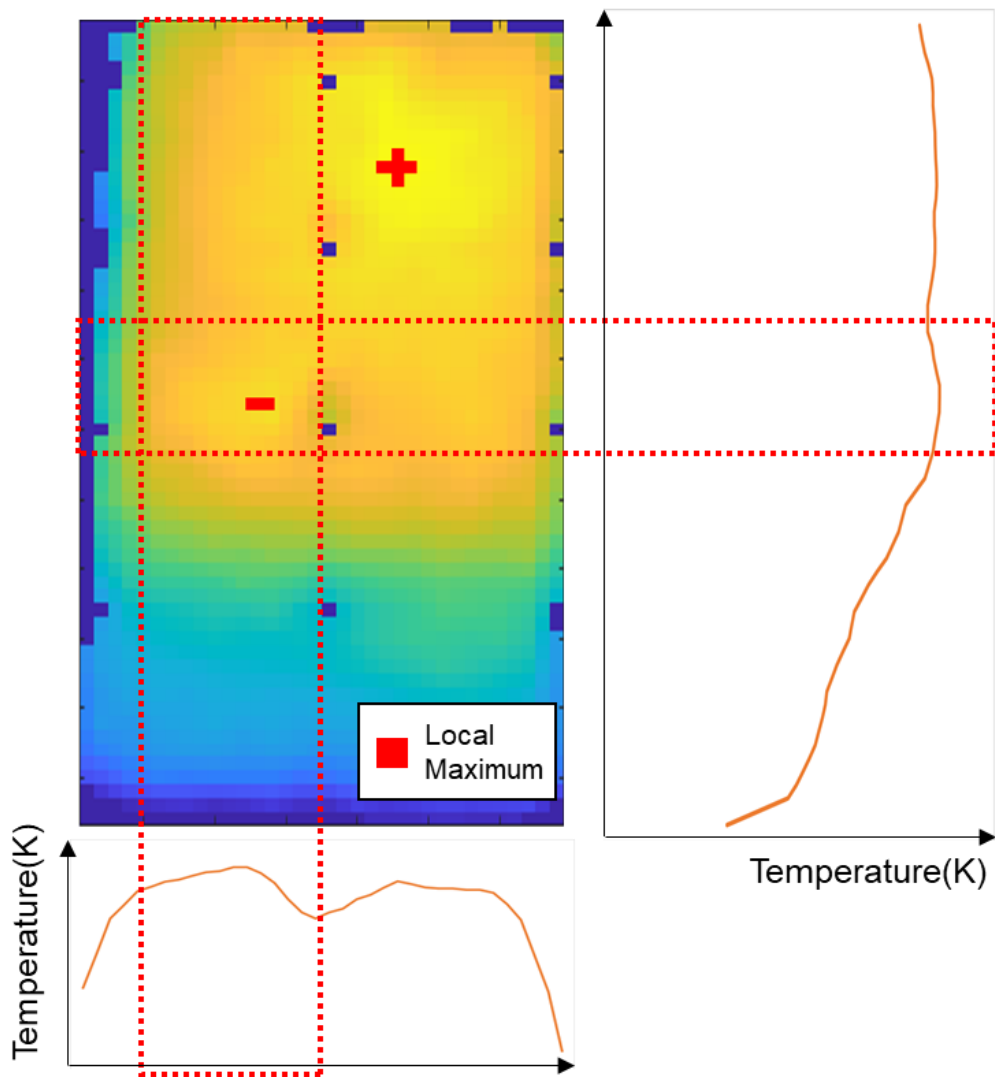


Fig. 5. Modified area detection

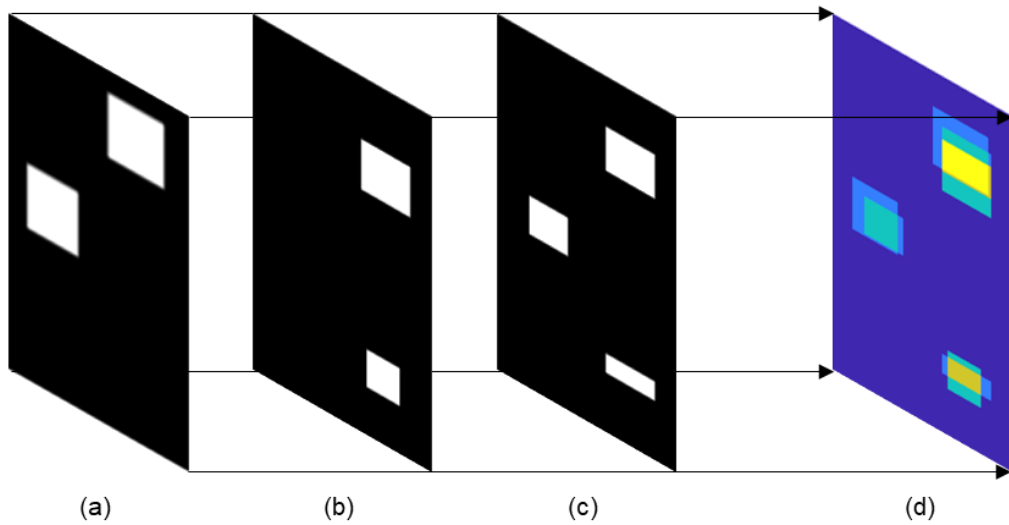


Fig. 6. Accumulation example



### 3. Field experiment

#### 3.1. Experimental setup

The performance of the proposed method was validated through a field experiment. To validate the applicability of the method to various protective materials, some cells on the PV panel surface were coated with three protective materials. Figure 7(a) shows the position of the coated cells for each protective material. A and B were coated with a spray-type protective material developed by different companies, and C was coated with a paraffin-based phase-change material.

A Parrot ANAFI thermal drone was used to acquire the thermal and visible images. The drone was equipped with a thermal imaging camera manufactured by Teledyne FLIR. The built-in thermal imaging camera can acquire thermal images with a resolution of  $160 \times 120$  over a temperature range of  $-10 \text{ }^\circ\text{C}$  to  $400 \text{ }^\circ\text{C}$ . In addition, the visible image acquired simultaneously with the thermal image had a resolution of  $3,264 \times 2,448$ . Figure 7(b) shows the drone used in the field experiment.



**Fig. 7.** Experimental setup (a) PV panel (b) drone

#### 3.2. Experimental results

To validate the performance of the proposed method, the PV panel was tested twice at different times and locations. The first experiment was performed on August 4, 2021 [Fig. 8(a)]. Infrared thermography images were acquired using the drone positioned at a height of 1 m from the ground and 3 m from the PV panel; 115 images were acquired continuously at a rate of 1 frame every 10 s. The second experiment was performed on August 30, 2021 [Fig. 8(b)]. Infrared thermography images were acquired using the drone positioned at a height of 1 m from the ground and 3.5 m from the PV panel; 82 images were acquired continuously at a rate of 1 frame every 10 s.



**Fig. 8.** Field experiment (a) first experiment (b) second experiment

Fig. 9(a) and Fig. 9(b) shows one of the thermal image sequences acquired in the first and second experiments, respectively. As argued earlier, the coated area having similar temperatures with surroundings cannot be explicitly visualized in the thermal images. Fig. 10(a) and Fig. 10(b) shows the results of applying the modified area detection method proposed in this study. In the figure, the yellow colour means a cell with a high possibility of being modified. The rectangle shown in the Fig. 10(c) represent actual cells modified with A, B, and C materials on the surface. As can be seen in the figure, all cells coated with protective material on the surface were detected as cells with a high probability of being protected.

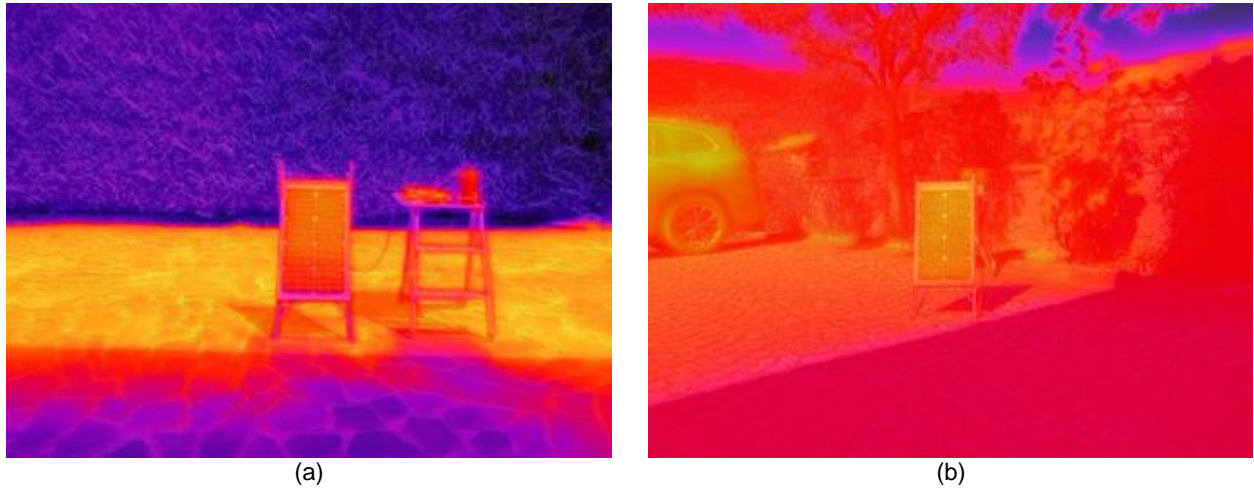


**Fig. 9.** Image acquired from field experiment (a) first experiment (c) second experiment

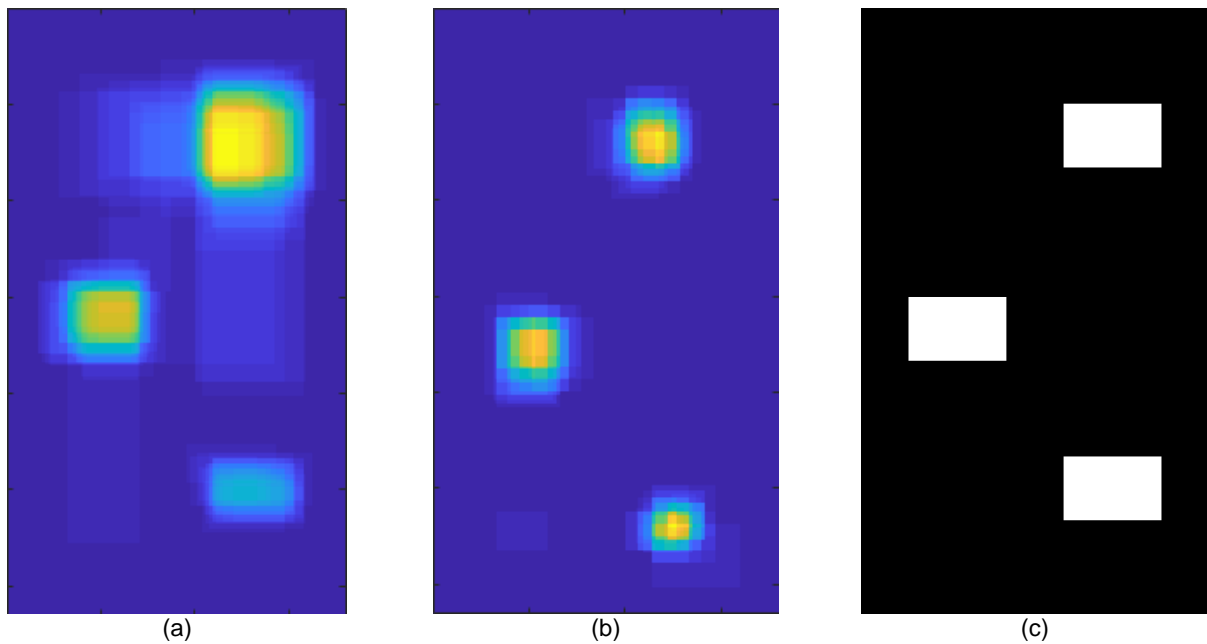


**Fig. 10.** Modified cell detection results (a) first experiment (b) second experiment (c) ground truth

#### 4. Conclusion

In this study, a method for detecting modified cells in a PV panel from thermal images acquired continuously using a drone was proposed. As a preprocessing step, the visible image was registered with the thermal image, and the thermal image was applied with a median filter. Thereafter, the PV cells were detected in the visible image. Subsequently, the local maximum pixel was identified in the PV cell and the modified area was detected. Finally, the modified area detection results of the individual images were accumulated. The modified cells detected in multiple thermal images were assumed to exhibit high protection potential. The results of this study showed that modified cells with a slight temperature difference among them can be automatically detected.

After detecting the local maximum pixel, the modified area was defined by applying a threshold value. The proposed threshold value was determined through two experiments. However, a method that changes automatically according to the environment is to be developed.

## ACKNOWLEDGEMENT

This study was supported by a National Research Foundation of Korea (NRF) grant that was funded by the Korean government (MSIP) (No. 2021R1A2C4002936). This research was supported by the National Research Foundation of Korea (NRF) grant funded by the Korea government (MSIP) (No. 2021R1A4A1031705). The authors would like to thank Mr. Mirco Guerrini (Caldo Continuo S.r.l., Ravenna, Italy) who provided the paraffin-based phase-change material (PCM) used in this work. The authors would like to also thank Eng. Massimo Cretarola who helped to build part of the experimental setup.

## REFERENCES

- [1] Lyu Y., Fairbrother A., Gong M., Kim J.H., Gu X., Kempe M., Julien S., Wan K.-T., Napoli S., Hauser A., O'Brien G., Wang Y., French R., Bruckman L., Ji L., Boyce K., Impact of environmental variables on the degradation of photovoltaic components and perspectives for the reliability assessment methodology, *Solar Energy*. – Vol. 199, no 15, 425-436, 2020.
- [2] Mon G., Wen L., Ross R., Adent D., Effects of temperature and moisture on module leakage currents, 18th IEEE PVSC. 1985.
- [3] Zahedi R., Ranjbaran P., Gharehpetia G.B., Mohammadi F., Ahmadihangar R., Cleaning of floating photovoltaic systems: A critical review on approaches from technical and economic perspectives, *Energies*. – Vol.14, 2018, 2021.
- [4] CHOOSE NANOTECH, <https://www.choosenano.com/choose-protects-solar-panels-and-improve-the-production-of-energy/>
- [5] CAMP Professional, <https://www.campitalia.it/professional/en/product/protect/>
- [6] AI Technology, <https://www.aitechnology.com/products/solar/solar-energy-coating/>
- [7] EziCleen, <https://www.ezicleen.com.au/services/solar-panel-protection/>
- [8] Deane S., Avdelidis N.P., Ibarra-Castanedo C., Zhang H., Nezhad H.Y., Williamson, A.A., Mackley T., Maldague X., Tsourdos A., Nooralishahi P., Comparison of Cooled and Uncooled IR Sensors by Means of Signal-to-Noise Ratio for NDT Diagnostics of Aerospace Grade Composites, *Sensors*. - Vol. 20, no 12, 3381, 2020.
- [9] Gallardo-Saavedra S., Hernández-Callejo L., Alonso-García M.D.C., Muñoz-Cruzado-Alba J., Ballestín-Fuertes J., Infrared Thermography for the Detection and Characterization of Photovoltaic Defects: Comparison between Illumination and Dark Conditions, *Sensors*. - Vol. 20, no 16, 4395, 2020.
- [10] Wang Q., Paynabar K., Pacella M., Online automatic anomaly detection for photovoltaic systems using thermography imaging and low rank matrix decomposition, *Journal of Quality Technology*. DOI: 10.1080/00224065.2021.1948372.